Ovarian Hormone-Induced Reorganization of Oxytocin-Labeled Dendrites and Synapses Lateral to the Hypothalamic Ventromedial Nucleus in Female Rats

Gerald D. Griffin,[1]* Sarah L. Ferri-Kolwicz,[2] Beverly A.S. Reyes,[3,4] Elisabeth J. Van Bockstaele,[3,4] and Loretta M. Flanagan-Cato[1,2]

[1]Neuroscience Graduate Group, University of Pennsylvania, Philadelphia, Pennsylvania 19104
[2]Department of Psychology, University of Pennsylvania, Philadelphia, Pennsylvania 19104
[3]Department of Neurosurgery, Thomas Jefferson University, Philadelphia, Pennsylvania 19107
[4]Farber Institute for Neurosciences, Thomas Jefferson University, Philadelphia, Pennsylvania 19107

ABSTRACT

Central oxytocin (OT) modulates many social behaviors, including female rat sexual receptivity, quantified as the copulatory stance known as lordosis. The expression of the lordosis response is modulated by OT action in the ventromedial nucleus of the hypothalamus (VMH), as demonstrated by behavioral pharmacology experiments. However, the subcellular localization of OT in this brain region has been unclear. We tested the hypothesis that ovarian hormones reorganize OT-labeled pre- or postsynaptic elements in the fiber complex lateral to the VMH by using immunoelectron microscopy. OT immunolabeling occurred in axonal boutons identified by the presence of small, clear synaptic vesicles and double labeling with the presynaptic markers synaptophysin and vesicular glutamate transporter 2. OT immunoreactivity also was observed in dendritic profiles, verified with double labeling for the dendrite-specific marker microtubule-associated protein 2. Ovarian hormones did not alter the density of axonal boutons; however, estradiol treatment reduced the density of dendritic profiles by 34%. This effect was reversed when progesterone was given subsequent to estradiol. The effect of estradiol treatment was specific to dendrites that lacked OT immunostaining; the density of OT-labeled dendritic profiles remained constant during estradiol treatment. With the estradiol-induced exit of non-OT-labeled dendritic profiles, the remaining OT-labeled dendritic profiles experienced an increase in their number of synaptic contacts. Thus, hormone treatments that mimic the 4-day rat estrous cycle provoke a chemically coded reorganization of dendrite innervation in the fiber plexus lateral to the VMH that may underlie the hormone-specific effect of OT on reproductive behavior. J. Comp. Neurol. 518:4531–4545, 2010.

INDEXING TERMS: axonal boutons; dendrites; estradiol; glutamate; immunoelectron microscopy; lordosis; microtubule-associated protein 2; neurohypophyseal tract; neuropeptide; progesterone; synaptophysin; vesicular glutamatergic transporter 2

Female rat reproductive behavior has been a useful model for the study of neural circuits that mediate mammalian motivated behavior. This hormone-dependent behavior is controlled by the ventromedial nucleus of the hypothalamus (VMH) (reviewed in Flanagan-Cato et al., 2001). Although the VMH is dense in neurons, very few afferents penetrate the nucleus (Millhouse, 1973a,b). Instead, axonal projections to the VMH from other brain regions encapsulate the nucleus (Luiten and Room, 1980; Kita and Oomura, 1982; Simerly and Swanson, 1988; Fahrbach et al., 1989). These axons, along with VMH dendrites, form a narrow shell around the VMH (Millhouse, 1973a). In addition, there is a lateral fiber complex (VMHlfc) situated near the VMH, including axons labeled for the neuropeptide oxytocin (OT) (O'Donohue et al.,

Grant sponsor: National Institutes of Health; Grant numbers: MH64371 and TG-MH017168.

*CORRESPONDENCE TO: Gerald D. Griffin, Department of Microbiology, University of Pennsylvania, 3610 Hamilton Walk, 302C Johnson Pavilion, Philadelphia, PA 19104-6241. E-mail: gdg@mail.med.upenn.edu.

Received October 6, 2009; Revised June 28, 2010; Accepted July 1, 2010
DOI 10.1002/cne.22470
Published online July 26, 2010 in Wiley Online Library (wileyonlinelibrary.com)

1979; Joseph et al., 1981; Palkovits, 1982; Watts et al., 1987; Daniels and Flanagan-Cato, 2000).

Activation of ovarian hormone receptors in the VMH (Pfaff and Keiner, 1973; Simerly et al., 1990; DonCarlos et al., 1991) exerts neurochemical changes that promote mating behaviors in synchrony with ovulation (Pfaff, 1989). The behavioral significance of OT receptors in the VMH was first suggested by the regulation of their expression by ovarian steroids (De Kloet et al., 1986; Coirini et al., 1989; Schumacher et al., 1990; Bale and Dorsa, 1995; Quinones-Jenab et al., 1997). Treatments that selectively disrupt OT receptor activity revealed that endogenous OT acts in the VMH to promote female sexual behavior in rats (Witt and Insel, 1991; McCarthy et al., 1994). Conversely, central application of exogenous OT enhances female receptivity (Arletti and Bertolini, 1985; Caldwell et al., 1986; Gorzalka and Lester, 1987). Although the regulation and function of the OT receptors in the VMH has been described, the subcellular localization of OT itself in the VMH is unclear.

At least three possible mechanisms have been proposed to explain the endogenous delivery of OT to its receptors in the VMH. First, OT may be released from the dendrites of distant OT neurons in the PVN and supraoptic nucleus (SON) and diffuse to the VMH (Morris and Pow, 1991; Sabatier et al., 2007). Dendritic release of OT in the PVN has been well documented (Ludwig and Pittman, 2003; see Landgraf and Neumann, 2004 for review). However, it remains unclear whether or not dendritically released OT sufficiently reaches receptors in the VMH. Second, OT may be released en passage from neurohypophyseal axons in the VMHlfc and diffuse toward receptors in the VMH. With these first two possible mechanisms, OT receptors in the VMH could be activated by the array of physiological stimuli that engage magnocellular OT neurons. Third, OT may be released within the confines of synaptic contact in the VMHlfc. Although the majority of these axons terminate in the posterior pituitary, some may form synapses in the fiber plexus. This third proposed mechanism allows for the possibility of OT receptor activation based on input selectively stimulated by mating cues.

The present study determined the subcellular localization of OT in the VMHlfc in adult ovariectomized rats administered vehicle or ovarian hormones. Immunogold labeling for OT was localized with electron microscopy based on both structural features and chemical markers, in particular, synaptophysin, vesicular glutamate transporter 2 (VGLUT2), and microtubule-associated protein 2 (MAP2). We then tested the hypothesis that ovarian hormones modulate the synaptic organization in the VMHlfc, particularly with regard to OT-labeled synaptic elements. The results confirm prior Golgi evidence that ovarian hormones have dynamic effects on dendrites in the VMHlfc (Griffin and Flanagan-Cato, 2008). In addition, we report two novel results: 1) that OT itself is found in some VMH dendrites; and 2) that the presence of OT in dendrites is associated with a unique pattern of ovarian hormone-induced synaptic reorganization.

MATERIALS AND METHODS

Animals

A total of nine adult Sprague-Dawley female rats (Taconic, Hudson, NY) were group housed in plastic tubs (41 × 21 × 22 cm) with standard bedding. Rat chow and tap water were available ad libitum. The colony temperature was maintained at 22°C, with a 12/12-hour reverse light/dark cycle, and with lights off at 1100 hours. After they had acclimated to the colony for 1 week, animals were bilaterally ovariectomized during general anesthesia (90 mg/kg ketamine and 9 mg/kg xylazine, both i.p.). Upon completion of the surgery, rats were given yohimbine (2.1 mg/kg, i.p.) to counteract the xylazine and, after a period of observation, were returned to their home cages. The Institutional Animal Care and Use Committee of the University of Pennsylvania approved all animal procedures. Dr. W. Scott Young (National Institute of Mental Health) generously provided brains from OT knockout mice (n = 2) and a wildtype littermate (n = 1) for use as controls for antibody labeling.

After 1 week of recovery from the ovariectomy, animals were randomly assigned to one of three hormone treatment groups: vehicle, estradiol benzoate (EB) alone, or EB combined with progesterone (EBP). These hormone regimens have been previously described (Griffin and Flanagan-Cato, 2008). Briefly, animals were administered two daily subcutaneous injections of sesame oil (vehicle) or 10 μg of 17-β—estradiol benzoate (Sigma, St. Louis, MO; both EB and EBP groups). Forty-eight hours later, the vehicle and EB groups were administered vehicle and the EBP group received 500 μg of progesterone (Sigma). All animals were deeply anesthetized 4 hours after the last injection and transcardially perfused through the ascending aorta with a series of solutions: 10 ml heparinized saline, 50 ml of 3.3% acrolein (Electron Microscopy Sciences, Fort Washington, PA), and 200 ml of 2% formaldehyde in 0.1 M phosphate buffer (pH 7.4). The brains were removed immediately after the perfusion fixation, and postfixed in the same fixative overnight at 4°C. Sections then were cut in the coronal plane (40 μm) by using a Vibratome (Technical Product International, St. Louis, MO) and collected into 0.1 M phosphate buffer.

Western blot

Thirty micrograms of protein from the rat cortex or mediobasal hypothalamus were loaded on a NuPAGE 4–12%

TABLE 1.
Primary Antibodies Used in This Study

Primary antibody	Immunogen	Cat. no.	Supplier	Dilution
Rabbit polyclonal oxytocin	Peptide sequence: H-Cys-Tyr-Ile-Gln-Asn-Cys-Pro-Leu-Gly-NH_2	T-4084	Bachem (King of Prussia, PA)	1:1,000
Mouse monoclonal synaptophysin	Full-length protein from crude human synaptic immunoprecipitate	MAB329, clone SP15	Millipore (Billerica, MA)	1:500
Mouse monoclonal vesicular glutamate transporter 2 (VGLUT2)	Whole recombinant VGLUT2 from rat	MAB5504, clone 8G9.2	Millipore	1:500
Mouse monoclonal microtubule-associated protein 2 (MAP2)	Rat brain MAPs	M4403, clone HM-2	Sigma (St. Louis, MO)	1:500

Bis-Tris gel (Invitrogen, Carlsbad, CA) and subsequently transferred to a polyvinylidene fluoride (PVDF) membrane. Next, the membrane was blocked in 5% dry milk and probed for VGLUT2 by using the mouse monoclonal anti-VGLUT2 antibody (MAB5504, clone 8G9.2; Millipore, Billerica, MA; 1:500 dilution). After a series of washes in phosphate-buffered saline (PBS), the PVDF membrane was then placed into ECL anti-mouse secondary antibody (GE Healthcare UK, Little Chalfont, UK; 1:3,000). Following thorough washing of the membrane, reagents from the Amersham ECL Plus Western Blotting Detection System (GE Healthcare UK) were placed directly onto the blot. Chemiluminescence was then detected by using the Image Reader LAS 1000 Pro software (Fujifilm, Tokyo, Japan). All samples were run in triplicate.

Antisera specificity

A list of all primary antibodies used is found in Table 1. The immunoelectron microscopy study used a polyclonal antibody generated in rabbit (T-4084; Bachem, King of Prussia, PA; 1:1,000 dilution) raised against the nonapeptide OT (H-Cys-Tyr-Ile-Gln-Asn-Cys-Pro-Leu-Gly-NH_2). Radioimmunoassay data provided by the manufacturer reported 100% and 0% cross-reactivity for OT and vasopressin, respectively. We performed additional specificity tests with light microscopy immunohistochemistry, as follows. Ovariectomized female rats were perfused, as previously described (Flanagan-Cato et al., 2006), and the brains were sectioned coronally (40 μm) by using a Vibratome. After incubation with the appropriate primary antibody, sections were placed in the following incubations, alternating with washes: biotinylated secondary anti-rabbit antibody (1:500, Jackson ImmunoResearch, West Grove, PA); avidin-biotin horseradish peroxidase (1:100, Vector Elite ABC kit, Vector Labs, Torrance, CA); and 3,3′-diaminobenzidine (0.2%) with hydrogen peroxide (0.025%, both from Sigma-Aldrich, St. Louis, MO).

OT-labeled fibers were easily discernable in the VMHlfc (Fig. 1A). As a positive control, the Bachem OT antibody provided robust labeling in the VMHlfc as well as the perikarya in the murine PVN, a known site of synthesis for the peptide in mammals (Fig. 1B,C). Negative controls included sections of the rat VMHlfc that underwent the normal labeling protocol with the omission of the primary antiserum. These sections exhibited no OT labeling in the VMHlfc (Fig. 1D). Likewise, rat VMHlfc sections exposed to OT antiserum preabsorbed with the OT peptide (2.5 mg/ml) also did not display OT labeling (Fig. 1E). Finally, brain sections from OT knockout mice failed to display OT immunoreactivity, unlike the sections from the wild-type littermate stained in parallel (Fig. 1F). After these positive and negative controls verified the specificity of the Bachem anti-OT antibody in this tissue, immunoelectron microscopy analysis of the rat VMHlfc was conducted with this antibody. All sections were counterstained with Cresyl Violet (Sigma).

The monoclonal primary antibody toward synaptophysin (MAB329, clone SP15; Millipore) reacted with synaptophysin expressed in CHO cells (information from manufacturer). This primary antibody recognizes a single band at the expected size of 38 kDa (Honer et al., 1993). Additionally, Navarro-Quiroga and colleagues (2006) demonstrated that labeling due to this primary antibody was restricted to synapses, the exclusive location of synaptophysin. The mouse monoclonal VGLUT2 antibody (MAB5504, clone 8G9.2; Millipore) recognized the expected single 56-kDa band on a Western blot of mouse brain lysates (10 μg of protein; information provided by the manufacturer; also see Fig. 2). Also, Wong and colleagues (2008) reported that this anti-VGLUT2 primary antibody revealed the known thalamocortical terminations in layer 4 of the cortex. The mouse monoclonal MAP2 antibody (M4403, clone HM-2; Sigma) was raised against rat brain MAPs and does not cross-react with other MAPs or tubulin (information provided by the manufacturer). Moreover, this primary antibody has been shown to specifically label somatodendritic regions of differentiated neurons (Lim et al., 2008) and detects discrete 280-kDa (expected for MAP2a and MAP2b) and 70-kDa bands (MAP2c; Cote et al., 1999).

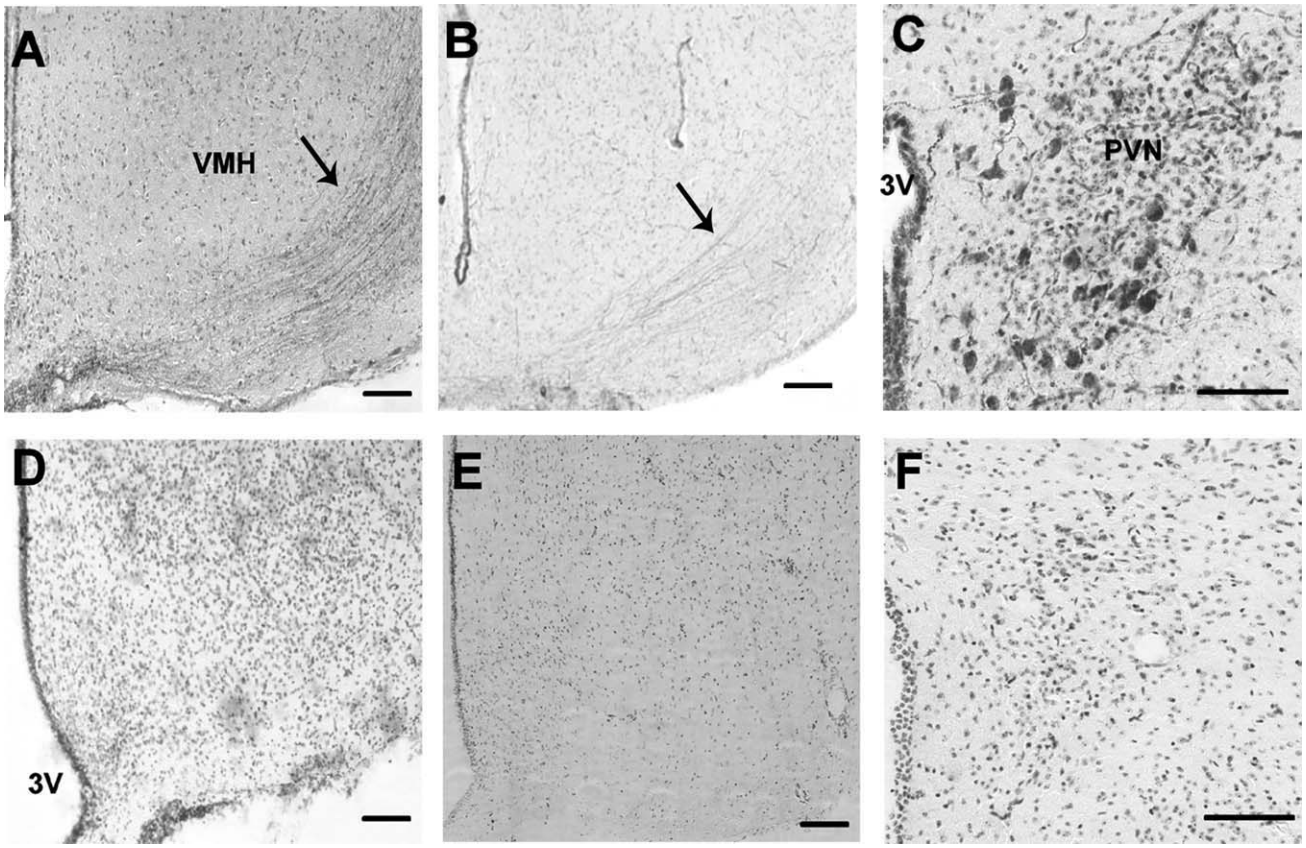

Figure 1. Light-microscopic-level photomicrographs illustrating the specificity of the anti-OT primary antibody used in the electron microscopy study. **A:** A coronal section including the ventromedial nucleus of the hypothalamus (VMH) from an ovariectomized rat incubated with the Bachem anti-OT antibody. Arrow indicates labeling of axonal fibers lateral to the VMH. **B,C:** A coronal section from a male wild-type mouse illustrating OT labeling in fibers lateral to the VMH (B) and in the paraventricular nucleus (PVN; C). **D:** A section not exposed to the Bachem primary antibody, but processed through all subsequent labeling steps, did not exhibit OT labeling adjacent to the VMH. **E:** A section co-incubated with the primary antibody and OT (2.5 mg/ml) did not display labeling of fibers lateral to the VMH. **F:** A coronal section from a male OT knockout mouse indicating a lack of OT labeling in the PVN. All sections were counterstained with Cresyl violet. 3V, third ventricle. Scale bar = 100 μm in A–F.

Immunoelectron microscopy

Coronal sections throughout the rostrocaudal extent of the VMH were processed for electron microscopic analysis after immunolabeling for OT only, or double labeling for OT with synaptophysin, VGLUT2, or MAP2. In double-labeled sections, immunoperoxidase labeling was used to identify synaptophysin, MAP2, or VGLUT2, whereas silver-intensified immunogold labeling was used to identify OT. Briefly, sections were placed for 30 minutes in 1% sodium borohydride in 0.1 M phosphate buffer (pH 7.4) to reduce amine-aldehyde compounds. For all incubations and washes, sections were continuously agitated with a rotary shaker. The tissue sections then were incubated in 0.5% bovine serum albumin in 0.1 M Tris-buffered saline (TBS; pH 7.6) for 30 minutes. After this incubation, thorough rinses in 0.1 M TBS were performed. Subsequently, sections were incubated in rabbit anti-OT (Bachem; 1:1,000 dilution) alone or in a cocktail containing mouse anti-synaptophysin (1:500 dilution), mouse anti-VGLUT2 (1:500 dilution), or mouse anti-MAP2 (1:500 dilution) in 0.1% bovine serum albumin. Sections were incubated for 15–18 hours on a rotary shaker at room temperature. The following day tissue sections were rinsed three times in 0.1 M TBS and incubated in biotinylated donkey anti-rabbit (1:400; Vector, Burlingame, CA) and biotinylated donkey anti-mouse (1:400; Vector) for 30 minutes followed by rinses in 0.1 M TBS. Next, sections were placed in an avidin-biotin complex (Vector) for 30 minutes. This antibody-enzyme complex was visualized by a 10-minute reaction in 3,3′-diaminobenzidine (0.22%; Sigma-Aldrich) and hydrogen peroxide (0.3%) in 0.1 M TBS.

After primary anti-OT incubations, sections were rinsed three times with 0.1 M TBS, followed by rinses with 0.1 M phosphate buffer and 0.01 M PBS, pH 7.4. Sections then were incubated in a 0.2% gelatin-PBS and 0.8% bovine serum albumin buffer for 10 minutes followed by incubation

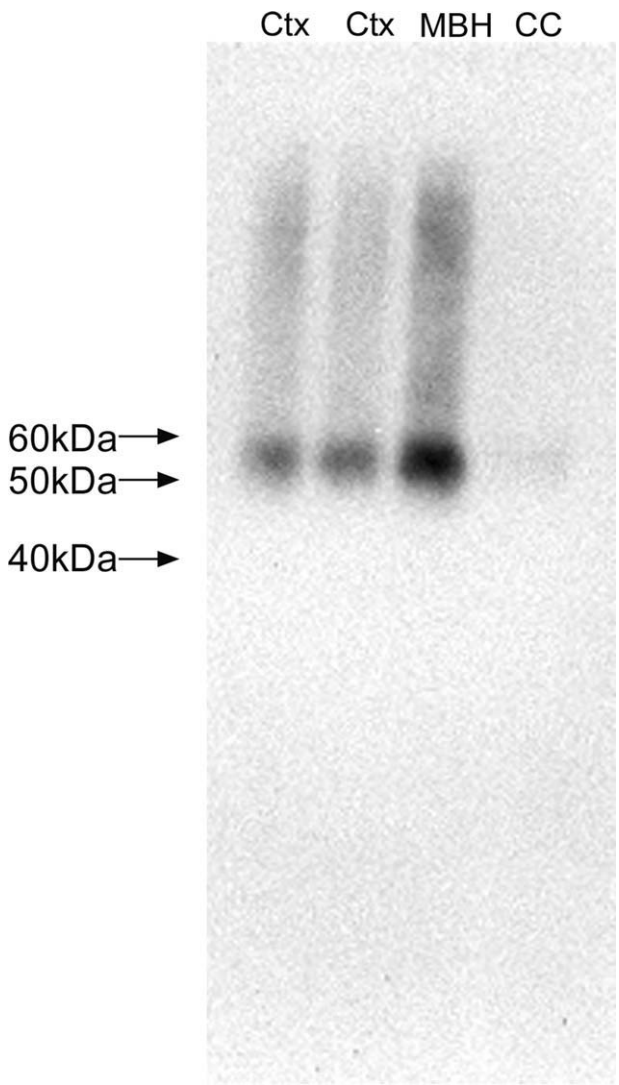

Figure 2. Western blot demonstrating the tissue specificity and appropriate molecular weight detection of the anti-VGLUT2 primary antibody employed for immunoelectron microscopy. The expected 56-kDa band was visualized from rat brain lysates from the mediobasal hypothalamus (MBH) and cortex (Ctx). Protein from the corpus callosum (CC) produced a faint band at the expected size for VGLUT2. Molecular weight markers are demarcated to the left of the blot.

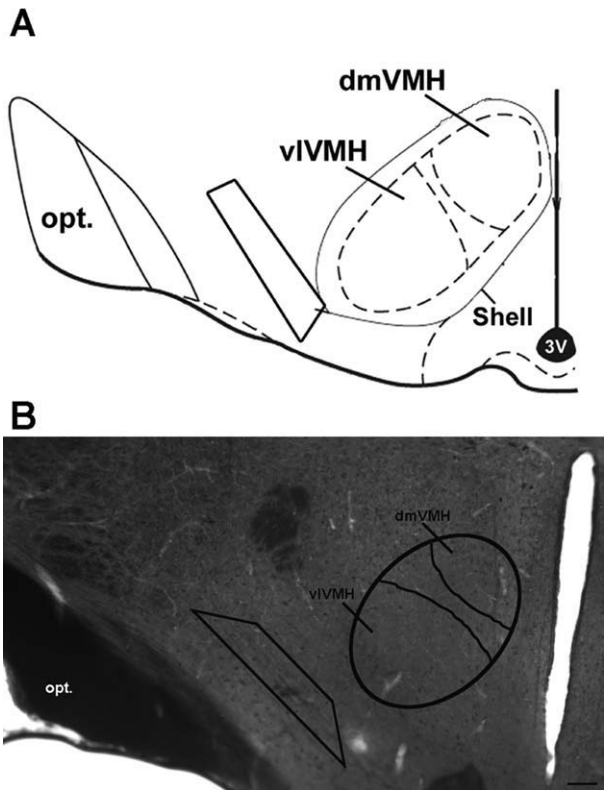

Figure 3. Diagram and photomicrograph illustrating the region that was analyzed at the ultrastructural level. **A:** An atlas drawing of the mediobasal hypothalamus, including the VMH. The trapezoid indicates the area that was analyzed with the electron microscope. **B:** A corresponding 40-μm section, immunolabeled with peroxidase for OT and treated with osmium tetroxide for ultrastructural analysis. A trapezoid has been superimposed on the OT fibers, indicative of the area of study. The approximate borders of the dorsomedial ventromedial nucleus of the hypothalamus (dmVMH) and ventrolateral VMH (vlVMH) are delineated. opt, optic tract; 3V, third ventricle. Scale bar = 100 μm in B.

in goat anti-rabbit immunoglobulin conjugated with 1-nm gold particles (Amersham Bioscience, Piscataway, NJ) at room temperature for 2 hours. Sections then were rinsed in buffer containing the same concentration of gelatin and bovine serum albumin, as above. After rinses with 0.01 M PBS, sections then were incubated in 2% glutaraldehyde (Electron Microscopy Sciences) in 0.01 M PBS for 10 minutes. Next, sections were washed in 0.01 M PBS and 0.2 M sodium citrate buffer (pH 7.4). A silver enhancement kit (Amersham Bioscience) was used to intensify the immunogold labeling. The optimal times for silver enhancement ranged between 10 and 15 minutes. Some tissue sections incubated for the detection of OT and synaptophysin or VGLUT2 were reverse-labeled such that OT was labeled with immunoperoxidase, and synaptophysin or VGLUT2 were labeled with silver-intensified immunogold to confirm a lack of cross-reactivity. After intensification, tissue sections were rinsed in 0.2 M citrate buffer and 0.1 M phosphate buffer and incubated in 2% osmium tetroxide (Electron Microscopy Sciences) in 0.1 M phosphate buffer for 1 hour, washed in 0.1 M phosphate buffer, dehydrated in an ascending series of ethanol followed by propylene oxide, and flat-embedded in Epon 812 (Electron Microscopy Sciences) on aclar (Electron Microscopy Sciences). Sections from all three groups were processed in parallel.

Coronal sections of the VMHlfc (Fig. 3) were cut with a diamond knife (Diatome-US, Fort Washington, PA) by using a Leica Ultracut ultratome at a thickness setting of

74 nm to obtain ultrathin sections. Images of the selected sections were compared with light microscopic images of the block face before sections were taken. Ultrathin sections were collected on copper mesh grids, examined with a Morgagni 268(D) transmission electron microscope (FEI, Hillsboro, OR), and digital images were captured by using the Advanced Microscopy Techniques (Danvers, MA) Advantage HR charge-coupled device (CCD) camera system. Figures were assembled and adjusted for brightness and contrast in Adobe Photoshop (San Jose, CA).

Additional controls and data analysis

Several controls were performed for the double-labeling experiments. First, sections processed in parallel but in the absence of the primary antibody directed against synaptophysin, VGLUT2, or MAP2 did not exhibit any detectable diaminobenzidine reaction product. Second, the lack of cross-reactivity between the labeling of each primary antiserum and the secondary antisera directed against the other concurrent primary antisera was verified by conducting the dual-labeling protocol but with the omission of one of the primary antisera.

For image analysis, digital images were obtained from the rostral and midrostral portions of the VMHlfc from all brains, all with good preservation of ultrastructural morphology. For each animal, three distinct 40-μm coronal sections were assayed. From each of these sections, four copper grids, spaced three grids apart and each containing three to four ultrathin sections, were analyzed. For the occasional case in which the appropriate grid was damaged, the next available grid was analyzed. Thus, 12 copper grids were analyzed per animal.

Images were captured with a range of objectives (22,000–44,000×). Figures were assembled and adjusted for brightness and contrast in Adobe Photoshop. Experimenters, blind to the hormonal status of individual animals, conducted the subcellular quantification. The inter-rater reliability was 0.91.

The cellular elements were identified based on the description of Peters and colleagues (1991). For example, somata were identified by a nucleus, Golgi apparatus, and smooth endoplasmic reticulum. Dendrites contained endoplasmic reticulum, were postsynaptic to axon terminals, and were larger than 0.7 μm in diameter. A terminal was considered to form a synapse if it showed a junctional complex or a restricted zone of parallel membranes with slight enlargement of the intercellular space, and/or was associated with postsynaptic thickening. Asymmetric synapses were identified by thick postsynaptic densities (Gray's type I); in contrast, symmetric synapses had thin densities (Gray's type II) both pre- and postsynaptically (Gray, 1959). The term "undefined" synaptic contact was used to denote parallel membrane association of an axon terminal plasma membrane juxtaposed to that of a dendrite or soma that lacked recognizable membrane specializations in the plane of section analyzed, and with no intervening glial processes.

Statistical analysis

For each animal, the quantification of ultrastructural features reflected the average values from three 40-μm sections, each of which included ultrathin sections from four separate copper mesh grids. A one-way ANOVA was used to compare the total area analyzed per animal. For all other parameters measured, a two-way ANOVA tested for a main effect and an interaction among hormone treatment, subcellular compartment, or the presence of OT labeling. If warranted, a Bonferroni-corrected t-test was employed for post hoc comparisons. Data are expressed as the mean (±SE). All statistical comparisons were performed by using the Prism 4.0 statistical software (GraphPad, San Diego, CA).

RESULTS

At the light microscopic level, a conspicuous stream of parallel OT-immunoreactive fibers could be observed in the VMHlfc (Fig. 1A). Given the proximity to the VMH, this region was targeted for electron microscopy analysis, as indicated by the trapezoid in Figure 3, to examine the subcellular localization of OT.

At the ultrastructural level, the VMHlfc contained a dense composition of intermingled unmyelinated axons, myelinated axons, synaptic boutons, dendrites, and glial processes. In a detailed analysis of micrographs from the vehicle-treated animals, 243 myelinated axon profiles, 1,239 axonal bouton profiles, and 1,744 dendritic profiles were analyzed. Cell bodies were sparse in this region, and blood vessels occasionally traversed the fiber plexus orthogonally, enveloped by endothelial cells. Gold/silver-labeled profiles, indicative of OT localization, were readily identified in single ultrathin sections. Consistent spatial organization of OT labeling was confirmed in serial sections, which further indicates that the observed labeling was not spurious.

As expected based on light microscopic level analysis, OT was present in myelinated axons, identified by the presence of microtubules, neurofilaments, and the characteristic myelin lamellae (Fig. 4A). Myelinated axons containing OT were common in areas of the VMHlfc that were dense with myelinated axons. OT was not observed in unmyelinated axons. Second, ultrastructural inspection revealed OT labeling in axonal boutons. Structural attributes, such as the presence of neurofilaments and

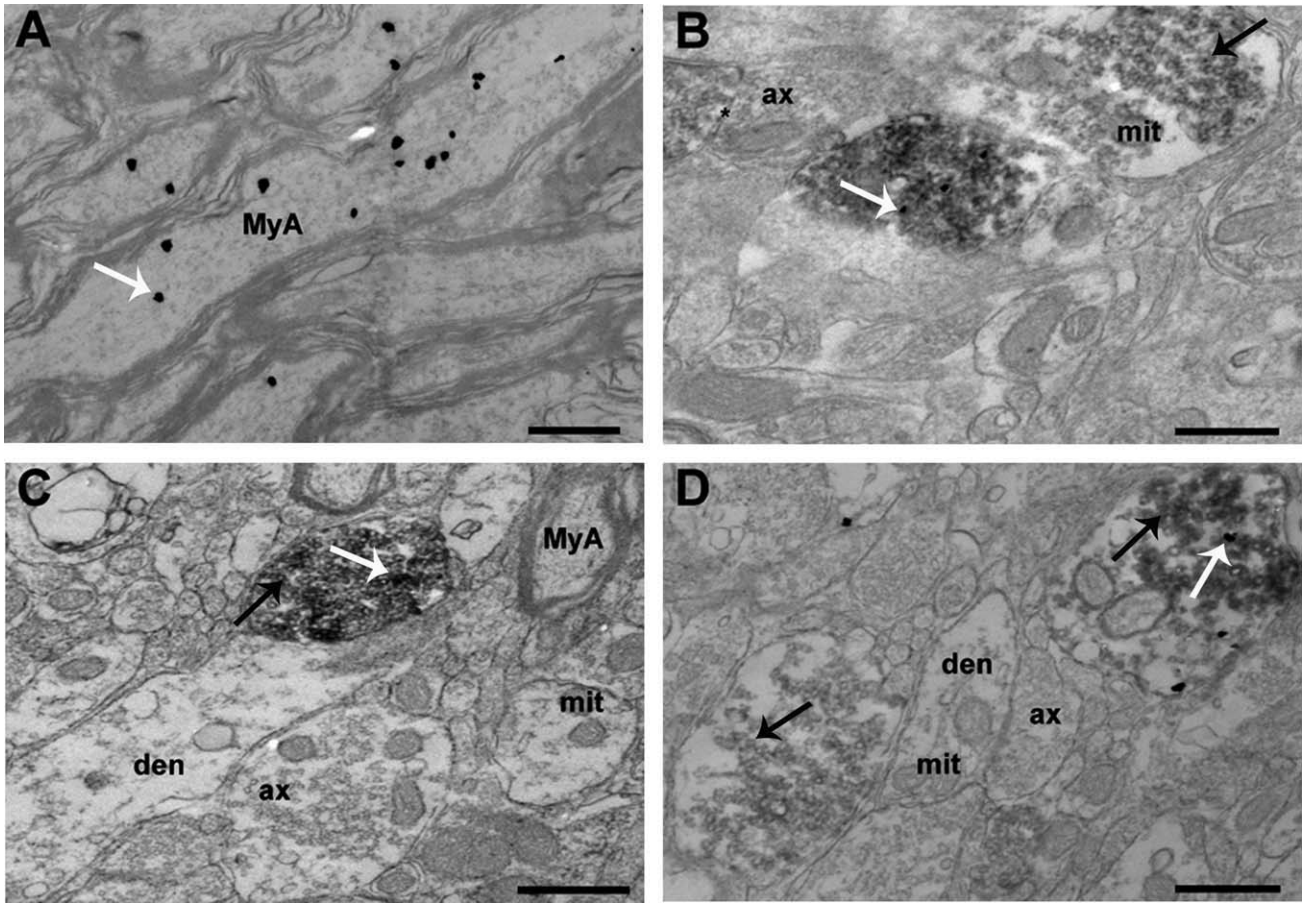

Figure 4. Electron photomicrographs illustrating OT labeling in myelinated axons and synaptic boutons. **A:** Certain regions within the fiber plexus were very dense in myelinated axons. Some of these myelinated axons contained marked amounts of immunogold particles, indicative of OT. **B:** The electron micrograph shows one axonal bouton containing only synaptophysin (dark, diffuse labeling indicated by black arrow). In the same micrograph, another bouton has labeling for OT (white arrow) in the midst of diffuse labeling for synaptophysin. The asterisk indicates a symmetric, axoaxonic synapse near boutons that contain OT and/or synaptophysin. **C:** Axonal boutons did not always contain VGLUT2 or OT. The white arrow indicates an OT-labeled immunogold particle whereas the black arrow denotes VGLUT2-labeled 3,3′-diaminobenzidine precipitate. Dendrites were always absent of labeling for VGLUT2. **D:** This micrograph shows one bouton with only VGLUT2 labeling (black arrow). Another axonal bouton is positive for both OT-labeled immunogold particles (white arrow) and VGLUT2-labeled 3,3′-diaminobenzidine precipitate (black arrow). ax, axon; den, dendrite; MyA, myelinated axon; mit, mitochondria. Scale bar = 500 nm in A–D.

synaptic vesicles in the absence of microtubules, signified axonal boutons. Often, these boutons contained mitochondria. Many axonal boutons made synaptic contact with dendrites or other axonal boutons. OT-labeled boutons were packed with small, clear synaptic vesicles; however, OT labeling was usually segregated from these vesicles (Fig. 4B). The occurrence of OT labeling in chemically defined boutons was confirmed with double labeling for the presynaptic marker synaptophysin. It should be noted that all boutons were immunopositive for synaptophysin, but not all were labeled for OT. In contrast, all structurally defined axonal boutons that were immunoreactive for OT also displayed concurrent synaptophysin staining.

In many cases, OT-immunoreactive axonal boutons could be observed to make asymmetric synaptic contacts with dendrites, suggestive of excitatory neurotransmission. To refine our characterization of OT-labeled synapses, double labeling with VGLUT2, a marker of glutamatergic vesicles, was performed (Fig. 4C,D). Only a subset of boutons was immunopositive for VGLUT2, and of these, only a subset was double-labeled with OT. However, OT labeling was only observed in boutons that also were labeled for VGLUT2.

A marked presence of OT was observed in some dendrites in the VMHlfc, recognized by the occurrence of microtubules, ribosomes, and mitochondria. Oxytocinergic labeling was found in both dendritic shafts and spines

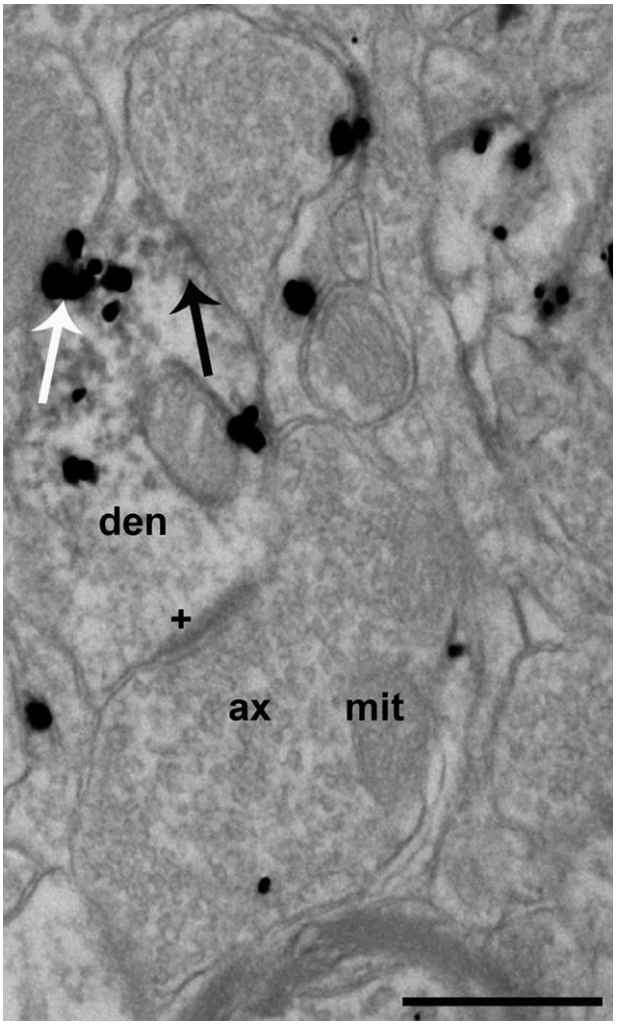

Figure 5. Electron photomicrograph of ultrathin sections immunolabeled for both OT and MAP2. OT-labeled immunogold particles (white arrow) were localized to dendrites that were immunopositive for MAP2 (black arrow, 3,3′-diaminobenzidine precipitate). Axonal boutons contained clear synaptic vesicles and were not labeled with MAP2 immunoreactivity. A dendrite that was labeled for OT and MAP2 received an asymmetric synapse (plus sign) from an axonal bouton that was also immunolabeled with OT. Ax, axonal bouton; den, dendrite; mit, mitochondria. Scale bar = 500 nm.

(Fig. 5). The occurrence of OT labeling in chemically defined dendrites was confirmed with double labeling for the dendrite-specific marker MAP2. Some dendrites double-labeled for MAP2 and OT were positioned at the postsynaptic side of asymmetric synapses.

Effect of ovarian hormones on general ultrastructural pattern

To investigate the effects of ovarian hormones on the synaptic organization of the VMHlfc, an average of 713.2 ($\pm$80.3) mm^2 were analyzed per animal, and the area examined per animal was equivalent across the three treatment groups (Fig. 6A). In all, 971 myelinated axons, 5,118 dendrites, and 3,858 axonal boutons were analyzed. Within this brain region, the density of dendritic profiles was significantly greater than that of axonal boutons or myelinated axons ($F_{(2,18)} = 135.5$; $P < 0.0001$); and axonal boutons were present at a higher density than myelinated axons ($P < 0.0001$). There was a marginally significant interaction ($F_{(4,18)} = 2.89$; $P = 0.052$) between hormone treatment and the density of these subcellular compartments. Specifically, estradiol treatment caused a marked reduction (34%) in the density of dendrites compared with vehicle-treated controls ($P < 0.05$). When the estradiol treatment was supplemented with progesterone, the dendrite density reverted to the level seen in vehicle-treated controls within 4 hours ($P < 0.05$). The densities of myelinated axons and axonal boutons were unaffected by these ovarian hormone treatments (Fig. 6B).

Distribution of OT labeling

Labeling for OT accounted for approximately 5–20% of axons, synaptic profiles and dendritic profiles, as depicted in Figure 7. OT labeling was found in a higher percent of axonal boutons and dendrites compared with myelinated axons, regardless of hormonal condition ($F_{(2,18)} = 9.389$; $P < 0.0016$; Fig. 6C).

In all treatment groups, the density of non-OT-labeled axonal boutons was much greater than those with the neuropeptide ($F_{(2,12)} = 174.2$; $P < 0.0001$). The density of boutons, whether containing OT or not, was not affected by hormone treatment (Fig. 7A). For axonal boutons that could be further identified as having the structural features of synaptic contact, the density was equivalent for synapses with and without OT labeling in the presynaptic compartment. Furthermore, hormone treatment did not affect the density of OT-positive or OT-negative synaptic profiles (Fig. 7B). Thus, for a bouton that did not contain OT, there was only a ~38% chance that it could be confirmed to make synaptic contact. In contrast, for a bouton that was immunopositive for OT, there was a nearly 100% chance it could be identified as having a postsynaptic partner.

The density of non-OT-labeled dendrites was markedly greater than those labeled with OT, with a ratio of approximately 7:1 ($F_{(2,12)} = 239.9$; $P < 0.0001$; Fig. 7C). As mentioned above, estradiol treatment caused an overall reduction in the density of dendritic profiles. There was a significant interaction between hormone treatment and the presence of OT in dendrites ($F_{(2,12)} = 4.946$; $P < 0.05$). In particular, hormone treatment had no effect on the density of dendrites labeled with OT. In contrast, estradiol treatment reduced the density of dendrites that

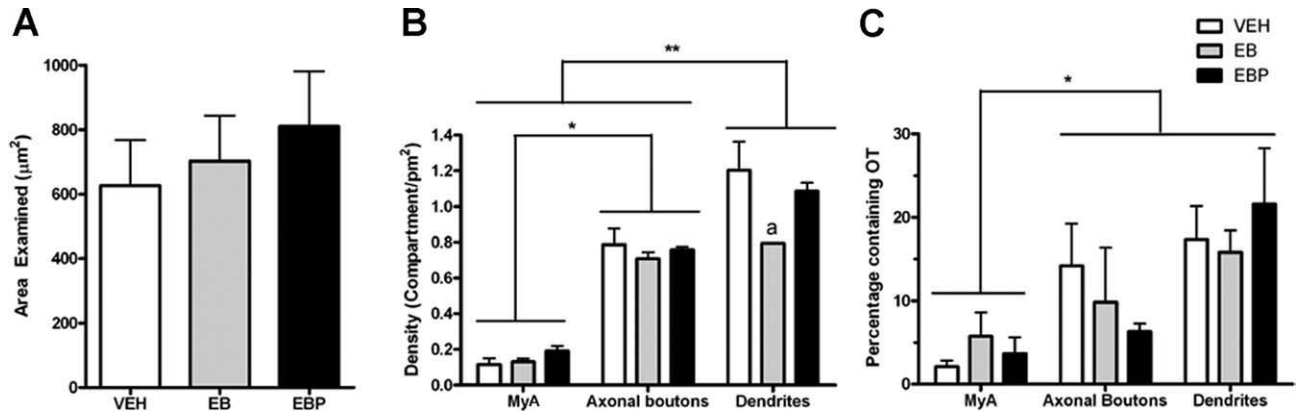

Figure 6. Bar graphs summarizing the total area analyzed, the density of various subcellular compartments, and the percentage of profiles that were immunolabeled for OT in each treatment group. **A:** The total area analyzed for each treatment group was similar. **B:** Within the area examined, the density of myelinated axons was less than that for axonal boutons, which, in turn, was less than dendritic profiles. Animals in the EB group had significantly lower densities of dendritic profiles than those in the VEH and EBP groups (denoted by "a"). **C:** There was no effect of hormonal treatment on the percent of myelinated axons, axonal boutons, and dendritic profiles that were labeled with OT. Overall, however, a higher percentage of axonal boutons and dendrites were immunolabeled for OT compared with myelinated axons. Brackets indicate differences in density or proportion between the categories of subcellular compartments. Level of significance is indicated by * ($P < 0.05$). Abbreviations: VEH, vehicle treatment; EB, estradiol benzoate treatment; EBP, estradiol benzoate and progesterone treatment; MyA, myelinated axon.

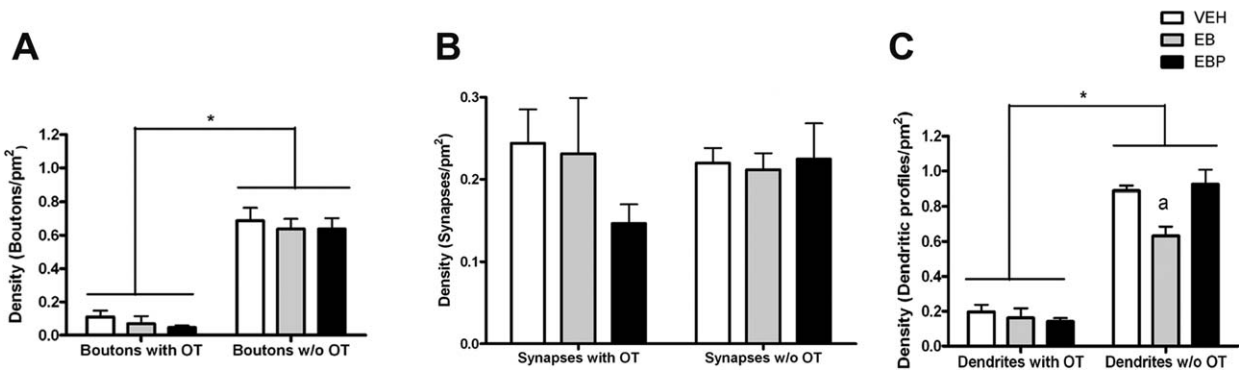

Figure 7. Bar graphs summarizing the density of boutons, synaptic profiles, and dendritic profiles according to whether they were negative or positive for OT immunolabeling. **A:** Ovarian hormone treatment had no effect on the density of axonal boutons, whether they were labeled with OT or not. There were significantly more unlabeled than OT-labeled axonal boutons. **B:** Of the subset of axonal boutons with clear structural characteristics of synaptic contact, ovarian hormone treatment had no effect on their density of axonal boutons, whether they were labeled with OT or not. There was an equivalent density of unlabeled and OT-labeled syanpses. **C:** There was an interaction between ovarian hormone treatment and labeling for OT on the density of dendritic profiles. There was a main effect of OT labeling, with unlabeled outnumbering OT labeled dendrites by approximately 7:1. Although ovarian hormone treatment had no effect on the density of OT-labeled dendritic profiles, estradiol treatment reduced the density of unlabeled dendritic profiles. The effect of estradiol was reversed by subsequent progesterone administration. Brackets indicate differences in density between the categories of subcellular compartments. Level of significance between OT labeling status is indicated by * ($P < 0.05$) and the effect of estradiol treatment on dendritic profile density, compared with vehicle and estradiol plus progesterone treatments, is indicated by "a" ($P < 0.05$). Abbreviations: VEH, vehicle treatment; EB, estradiol benzoate treatment; EBP, estradiol benzoate and progesterone treatment.

were not labeled for OT by 29% compared with vehicle ($P < 0.05$). The administration of progesterone reversed this decrease within 4 hours ($P < 0.05$).

It was intriguing that the density of dendritic profiles was reduced by estradiol treatment, in particular, in those without OT labeling, considering that the density of synaptic profiles remained unchanged by hormone condition. To better understand this result, the number of synaptic profiles per dendrite was quantified for all groups, taking into account whether or not the dendrite was labeled for OT. As shown in Figure 8A, there was a main effect of the presence of OT in the dendrite ($F_{(2,12)} = 39.89$; $P <$

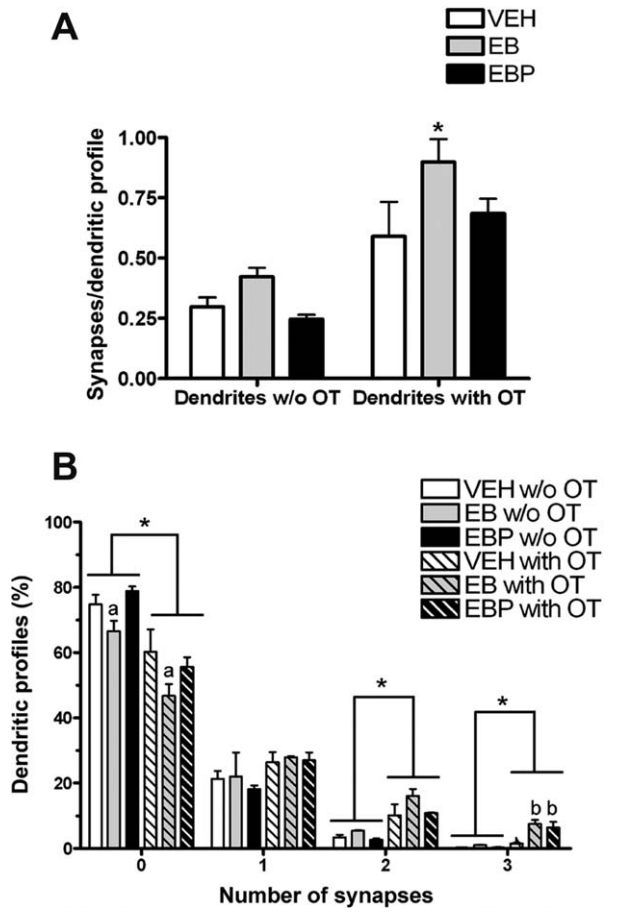

Figure 8. Bar graph and histogram summarizing the interaction between the presence of OT in dendritic profiles, ovarian hormone treatment, and the number of synapses per dendritic profile. **A:** There was a main effect on the average number of synapses per dendritic profile, with OT-labeled dendritic profiles receiving approximately twice as many inputs as non-OT labeled dendritic profiles. Although ovarian hormones did not alter the level of input to the non-OT labeled dendritic profiles, estradiol treatment increased the number of synaptic contacts per OT-labeled dendritic profile by approximately 51%. Progesterone treatment reversed the effect of estradiol. **B:** The histogram illustrates that dendritic profiles with or without OT most commonly were observed to receive no synaptic terminals. OT-labeled dendrites were less likely to have zero synaptic inputs, and more likely to have two synaptic inputs, compared with unlabeled dendritic profiles. Ovarian hormone treatment did not shift the distribution of innervation density for unlabeled dendritic profiles. However, for the OT-labeled dendritic profiles, estradiol treatment increased the percentage that received two or three synaptic contacts. Brackets indicate a main effect of OT-labeled versus non-OT labeled dendrites. Level of significance is indicated by * ($P < 0.05$). Significant effects of ovarian hormones treatments compared with vehicle are indicated by "a" ($P < 0.05$, less than vehicle) and "b" ($P < 0.05$, more than vehicle). Abbreviations: VEH, vehicle treatment; EB, estradiol benzoate treatment; EBP, estradiol benzoate and progesterone treatment.

0.0001) and a main effect of hormonal condition ($F_{(2,12)} = 4.653$; $P = 0.0319$). More specifically, the dendritic profiles labeled with OT received nearly twice as many synapses than dendritic profiles that were absent OT labeling. Furthermore, although estradiol treatment was associated with the removal of many of these dendritic profiles, the unlabeled dendrites remaining displayed no change in their average synaptic input after ovarian hormone treatment. For the OT-labeled dendritic profiles, although estradiol treatment did not alter their density, it increased the number of synaptic contacts per dendritic profile by approximately 51% ($P < 0.05$). Figure 8B illustrates the distribution of the number of synaptic contacts per dendritic profiles. A significantly higher proportion of non-OT-labeled dendrites had zero synaptic contacts compared with the OT-labeled dendrites (approximately 73% versus 54% overall [$F_{(2,12)} = 36.93$; $P < 0.0001$]). Conversely, a significantly lower proportion of non-OT labeled dendrites had one (20% versus 27%), two (4% versus 12%), or three (0.5% versus 5%) synaptic contacts compared with the OT-labeled dendrites ($F_{(2,12)} = 5.018$, 38.53, and 36.93, respectively ($P = 0.0448$, <0.0001, and <0.0001, respectively). Estradiol treatment further increased the percent of OT-labeled dendritic profiles that received three synaptic contacts compared with vehicle treatment ($P < 0.001$).

Given the subjective observation that the location of immunogold-labeled OT in synaptic boutons was segregated from the small clear vesicles that aggregate near the synaptic junction, the distance from the immunogold-labeled OT to the nearest synaptic junctional membrane versus the nearest plasma membrane was measured. As shown in Figure 9, there was a main effect of subcellular compartment ($F_{(1,8)} = 16.41$; $P = 0.0037$), i.e., OT-conjugated immunogold particles were found closer to both types of membranes in axonal boutons compared with dendritic profiles. In addition, there was a main effect of the membrane region ($F_{(1,8)} = 183.8$; $P < 0.0001$), with the OT-conjugated immunogold particles situated substantially closer to a nonsynaptic region of membrane compared with the nearest synaptic membrane. Ovarian hormone treatment did not significantly alter the location of OT-labeled particles within the axonal boutons. However, in dendrites OT-labeled particles were found closer to a synapse in the progesterone-treated group compared with the vehicle-treated group ($P < 0.02$).

DISCUSSION

This study had two major goals: 1) to localize OT within subcellular compartments of the VMHlfc; and 2) to test the hypothesis that ovarian hormones reconfigure the synaptic organization in the VMHlfc, especially OT-labeled elements. A solid body of literature demonstrates structural plasticity in the VMH itself (Carrer and Aoki, 1982; Nishizuka and Pfaff, 1989; Frankfurt et al., 1990; Calizo

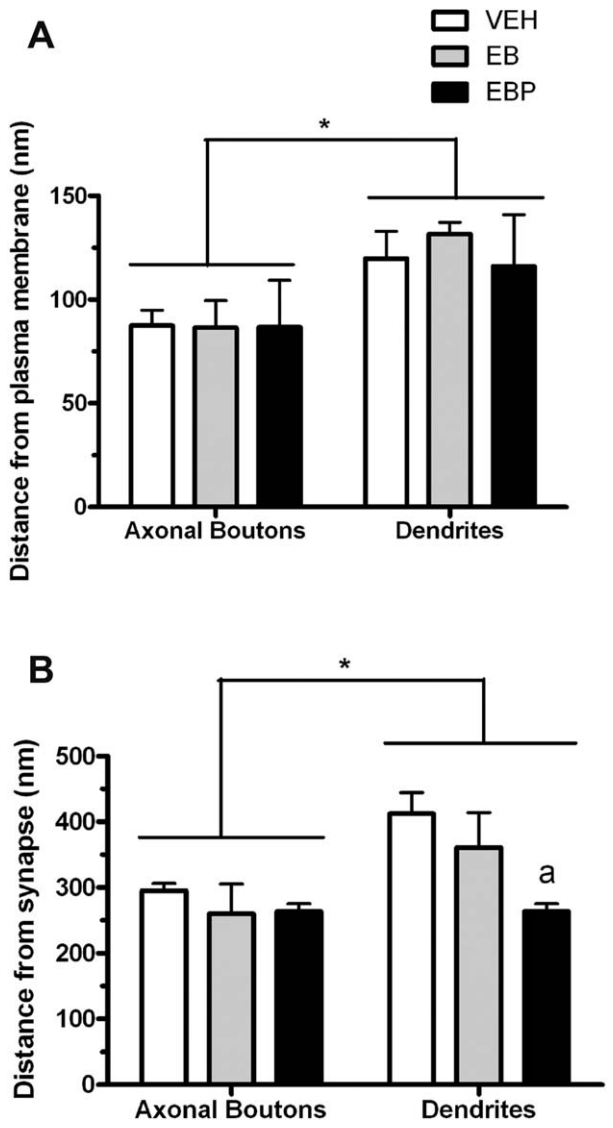

Figure 9. Bar graphs comparing the distance between OT-labeled immunogold particles and the nearest synaptic membrane versus nonsynaptic membrane in axonal boutons and dendritic profiles. The OT-conjugated immunogold particles were situated substantially closer to a nonsynaptic region of membrane compared with the nearest synaptic membrane in both axonal boutons and dendrites. In addition, OT-conjugated immunogold particles were found closer to either type of membrane in axonal boutons compared with dendritic profiles, as indicated by brackets. *, $P < 0.05$. "a" above bars, after progesterone treatment, OT labeling was found closer to synaptic membranes in dendrites than those in the vehicle condition ($P < 0.05$). Abbreviations: VEH, vehicle treatment; EB, estradiol benzoate treatment; EBP, estradiol benzoate and progesterone treatment.

and Flanagan-Cato, 2000; Madiera et al., 2001); however, the adjacent fiber field had not been investigated. This first ultrastructural study of the VMHlfc detected OT in axonal boutons, defined both structurally and with synaptophysin co-localization. OT-labeled axonal boutons were also immunopositive for VGLUT2. Although this structural study localized OT to boutons in the VMHlfc, we cannot state that the OT was synaptic in nature. In fact, given the distance over which OT-labeled immunogold particles were noted in boutons, it is very likely that release of OT is not occurring at the synapse. Unexpectedly, OT labeling was found in dendrites, as confirmed with co-localization with MAP2. Estradiol treatment markedly decreased the density of dendritic profiles in the VMHlfc. This effect was reversed within 4 hours of progesterone exposure, in striking accordance with Golgi impregnation analysis of long primary dendrites that ramify from VMH neurons (Griffin and Flanagan-Cato, 2008). This estradiol-induced reduction in dendrite availability was specific to dendrites that did not contain OT. Finally, estradiol treatment specifically increased the number of synapses per dendritic profile for OT-labeled dendrites without changing the level of input for unlabeled dendrites. These last two results suggest that dendritic labeling for OT signifies a unique dendrite function within the neural circuitry. Taken together, these results provide new clues about the synaptic organization of a behaviorally important peptide in the VMHlfc.

Ultrastructure of the VMHlfc

This study demonstrates that OT is localized within axonal boutons in the VMHlfc. Confocal microscopy analysis revealed that dendrites extending from the VMH made close contact with OT-labeled fibers in the VMHlfc (Daniels and Flanagan-Cato, 2000). Within OT-labeled boutons, small clear vesicles were aligned with the junctional zone, whereas OT was in proximity to a nonsynaptic portion of the bouton membrane. This subcellular localization provides structural evidence that OT, like other neuropeptides, may be released parasynaptically (Magistretti and Morrison, 1988; Conde, 1992; De-Miguel and Trueta, 2005). This is also the first report to demonstrate that axons in the fiber plexus form synapses with dendrites likely extending from the VMH, as first suggested by Millhouse based on Golgi analysis (Millhouse, 1973a). Thus, parasynaptic release of OT from axonal boutons in the VMHlfc may provide a temporally and spatially precise means for OT to regulate female sexual receptivity. The presence of OT in boutons in the VMHlfc does not preclude concomitant effects of more distant sources of OT, such as dendritic release from the PVN and/or SON, as proposed previously (Morris and Pow, 1991; Sabatier et al., 2007). It is possible that background levels of extracellular OT, triggered by various physiological stimuli that cause dendritic release, affect OT receptors in concert with locally released OT. Interactions between tonic and phasic effects of OT in the VMH warrant further study.

We have provided novel direct evidence that OT in the VMHlfc is co-localized with glutamate (Gray, 1959). OT and VGLUT2 have been co-localized in dendrites of neurons in the SON, a site of OT synthesis and dendritic release (Ludwig and Pittman, 2003; Ponzio et al., 2006). Exogenous OT increases the firing rate of VMH neurons (Kow et al., 1991). Endogenous OT may be released parasynaptically to activate VMH dendrites; however, possible interactions with glutamate in OT-induced excitability in the VMH remain unexplored.

Ultrastructure and MAP2 labeling confirmed the presence of OT in dendrites in the VMHlfc. These dendrites may arise from OT-producing neurons in the VMH. However, neither OT mRNA nor the peptide itself has been reported in soma in the VMH, the present study included. Second, dendrites from the SON and/or PVN, where OT cell bodies reside, could extend into this region. OT is trafficked into and released from dendrites, in conjunction with glutamate; thus the PVN and SON oxytocinergic dendrites also express VGLUT2 (Ponzio et al., 2006). Dendrites in the SON have been reported to be as long as 400 μm (Stern and Armstrong, 1998). However, this scenario is contradicted by the lack of VGLUT2 labeling in OT-containing dendrites in the VMHlfc. Thus, it seems unlikely that the dendrites that exhibit OT labeling arise from the PVN or SON.

A third scenario is that OT may be released from nearby boutons and then transported into dendrites for catabolism. Previous immunohistochemical work has shown that a primary antibody directed against OT also recognized the deamidated form of the peptide (Ivell et al., 1983). Supporting this notion is the labeling of OT in endosome-like vesicles in dendrites. The presence of OT in these organelles in dendrites may indicate that the peptide is internalized with the OT receptor. In HEK293T cells, OT receptors did not enter lysosomes but were packaged to be returned to the cellular membrane (Conti et al., 2009). Thus, the labeling we observed in dendrites may represent a combination of intact and partially degraded OT along with its receptor waiting to be recycled to the cell surface.

Beyond the VMH, OT receptors are found in a variety of other brain regions (Elands et al., 1988; Freund-Mercier et al., 1987; Tribollet et al., 1988; Yoshimura et al., 1993). In most cases, OT fibers have been identified in the same areas (Buijs, 1978; Swanson et al., 1980; Sofroniew and Schrell, 1981). In the well-studied dorsal vagal complex, OT has been localized to presynaptic boutons where it selectively increased the probability of glutamate release (Peters et al., 2008). OT-glutamate co-transmission has been noted previously (Hrabovszky et al., 2006; Ponzio et al., 2006). The fact that OT axonal projections target multiple brain regions that express OT receptors suggests that release from boutons may be a common mechanism of OT delivery.

Effect of ovarian hormones on VMH dendrites

The dendritic tree of VMH neurons includes a single long primary dendrite (LPD) extending in the ventrolateral direction to form a lattice with a lateral afferent fiber field (Millhouse, 1973a,b; Calizo and Flanagan-Cato, 2000). Ovarian hormones dynamically regulate these LPDs, with an estradiol-induced retraction that is reversed with combined progesterone treatment (Griffin and Flanagan-Cato, 2008). Taken together, these two studies suggest that the shortened LPDs are vacating the VMHlfc.

Several other paradigms indicate the importance of the LPD extension from the VMH into the VMHlfc in rats. Food-deprived male rats displayed 31% reduction in LPD length of their VMH neurons compared with ad libitum fed controls (Flanagan-Cato et al., 2008). Likewise, rats with a genetic tendency to gain weight on a high-energy diet also exhibited shorter LPDs compared with rats that resist such weight gain (LaBelle et al., 2009). The present results suggest that physiological conditions that reduce the LPD length of VMH neurons are associated with a rewiring of synaptic inputs to the remaining dendrites in the VMHlfc. However, the behavioral significance of the dendrite retraction is not clear in these conditions, and it may be that the re-partnering of the synaptic inputs is more critical than the retreat of dendrites.

The underlying cellular mechanism that mediates the estradiol-induced retraction, and progesterone-induced restoration, of LPDs requires further study. Neurons that express the nuclear estrogen receptor (ER)-α , and estradiol-induced progestin receptors are abundant in the VMH (Pfaff and Keiner, 1973; Simerly et al., 1990; Don-Carlos et al., 1991) and have well-documented genotropic effects on mating behavior (Rainbow et al., 1982; Glaser and Barfield, 1984; Meisel and Pfaff, 1984). In addition, estradiol has membrane-directed effects in this brain region (Kow and Pfaff, 2004). Furthermore, OT neurons in the PVN express ER-β, especially the parvocellular neurons in the medial subnucleus (Hrabovszky et al., 1998, 2004). Sakamoto and colleagues (2007) demonstrated that the G-protein-coupled membrane estrogen receptor GPR30 was present in the neurosecretory axonal swellings in the neurohypophysis. Thus, the site of hormone action could be pre- or postsynaptic, or both, and such action could occur through multiple receptor mechanisms. An intriguing aspect of both the Golgi and the ultrastructural analysis was that progesterone returned dendrite parameters to their values during the vehicle condition. This reversal by progesterone has been

seen in other types of estradiol-induced neural plasticity (Mills et al., 2004). The progesterone-induced proximity of dendritic OT to the postsynaptic membrane may be indicative of recent release and uptake.

A key finding in the current study was that ovarian hormones caused a rearrangement of synaptic connections in the VMHlfc. Estradiol treatment increased input to the OT-containing dendrites. Thus, the overall level of synapses remained constant in the face of retreating dendrites. A question for future study is whether the new synapses on the OT-labeled dendrites are inhibitory or excitatory. Likewise, factors remain to be identified that are differentially expressed in dendrites with and without OT that allow for this synaptic reorganization.

In conclusion, this first ultrastructural analysis of the VMHlfc characterized OT in glutamatergic boutons and dendrites. Several aspects of the results were unexpected and warrant future studies. Given the structural evidence that OT is released parasynaptically, it is unclear whether the OT receptors are located on the post-bouton dendrites and/or on other nearby dendrites. The biological basis of ovarian hormone-dependent mating behavior may include OT-mediated modulation of glutamate action. Although the significance of OT immunoreactivity in dendrites is not clear, it was indicative of dendrites sparing the estrogen-induced dendrite exodus from this region. The apparent lack of a hormone-induced change in the average density of presynaptic terminals obscured a rearrangement of connectivity, with OT-containing dendrites partnering with additional terminals during estradiol treatment. Overall, these results set forth striking new insights regarding the neural circuitry of the broader VMH area, particularly with regard to the presence of the behaviorally relevant neuropeptide OT.

ACKNOWLEDGMENTS

The authors thank Dr. Catherine S. Woolley for extensive helpful discussions, Dr. W. Scott Young for generously providing OT knockout mice and a wild-type littermate to determine the specificity of the OT antibody, and Neelam Shah and Jacques Beauvais for their excellent technical assistance.

LITERATURE CITED

Arletti R, Bertolini A. 1985. Oxytocin stimulates lordosis behavior in female rats. Neuropeptides 6:247–253.

Bale TL, Dorsa DM. 1995. Sex differences in and effects of estrogen on oxytocin receptor messenger ribonucleic acid expression in the ventromedial hypothalamus. Endocrinology 136:27–32.

Buijs RM. 1978. Intra- and extrahypothalamic vasopressin and oxytocin pathways in the rat. Cell Tissue Res 192:423–435.

Caldwell JD, Prange AJ, Pedersen CA. 1986. Oxytocin facilitates the sexual receptivity of estrogen-treated female rats. Neuropeptides 7:175–189.

Calizo LH, Flanagan-Cato LM. 2000. Estrogen selectively induces dendritic spines within the dendritic arbor of rat ventromedial hypothalamic neurons. J Neurosci 20: 1589–1596.

Carrer HF, Aoki A. 1982. Ultrastructural changes in the hypothalamic ventromedial nucleus of ovariectomized rats after estrogen treatment. Brain Res 27:221–233.

Coirini H, Schumacher M, Flanagan LM, McEwen BS. 1991. Transport of estrogen-induced oxytocin receptors in the ventromedial hypothalamus. J Neurosci 11:3317–3324.

Conde H. 1992. Organization and physiology of the substantia nigra. Exp Brain Res 88:233–248.

Conti F, Sertic S, Reversi A, Chini B. 2009. Intracellular trafficking of the human oxytocin receptor: evidence of receptor recycling via a Rab4/Rab5 "short cycle". Am J Physiol Endocrinol Metab 296:E532–E542.

Cote F, Do TH, Laflamme L, Gallo JM, Gallo-Payet N. 1999. Activation of the AT(2) receptor of angiotensin II induces neurite outgrowth and cell migration in microexplant cultures of the cerebellum. J Biol Chem 274:31686–31692.

Daniels D, Flanagan-Cato LM. 2000. Functionally-defined compartments of the lordosis neural circuit in the ventromedial hypothalamus in female rats. J Neurobiol 45:1–13.

De Kloet ER, Voorhuis DAM, Boschma Y, Elands J. 1986. Estradiol modulates density of putative 'oxytocin receptors' in discrete rat brain regions. Neuroendocrinology 44:415–421.

De-Miguel FF, Trueta C. 2005. Synaptic and extrasynaptic secretion of serotonin. Cell Mol Neurobiol 25:297–312.

DonCarlos LL, Monroy E, Morrell JI. 1991. Distribution of estrogen receptor-immunoreactive cells in the forebrain of the female guinea pig. J Comp Neurol 305:591–561.

Elands J, Beetsma A, Barberis C, de Kloet ER. 1988. Topography of the oxytocin receptor system in rat brain: an autoradiographical study with a selective radioiodinated oxytocin antagonist. J Chem Neuroanat 1:293–302.

Fahrbach SE, Morrell JI, Pfaff DW. 1989. Studies of ventromedial hypothalamic afferents in the rat using three methods of HRP application. Exp Brain Res 77:221–233.

Flanagan-Cato LM, Calizo LH, Daniels D. 2001. The synaptic organization of VMH neurons that mediate the effects of estrogen on sexual behavior. Horm Behav 40:178–182.

Flanagan-Cato LM, Calizo LH, Griffin GD, Lee BJ, Whisner SY. 2006. Sexual behaviour induces the expression of activity-regulated cytoskeletal protein and modifies neuronal morphology in the female rat ventromedial hypothalamus. J Neuroendocrinol 18:857–864.

Flanagan-Cato LM, Fluharty SJ, Weinreb EB, LaBelle DR. 2008. Food restriction alters neuronal morphology in the hypothalamic ventromedial nucleus of male rats. Endocrinology 149:93–99.

Frankfurt M, Gould E, Woolley CS, McEwen BS. 1990. Gonadal steroids modify dendritic spine density in ventromedial hypothalamic neurons: a Golgi study in the adult rat. Neuroendocrinology 51:530–535.

Freund-Mercier MJ, Stoeckel ME, Palacios JM, Pazos A, Reichhart JM, Porte A, Richard P. 1987. Pharmacological characteristics and anatomical distribution of [3H]oxytocin-binding sites in the Wistar rat brain studied by autoradiography. Neuroscience 20:599–614.

Glaser JH, Barfield RJ. 1984. Blockade of progesterone-activated estrous behavior in rats by intracerebral anisomycin is site specific. Neuroendocrinology 38:337–343.

Gorzalka BB, Lester GLL. 1987. Oxytocin-induced facilitation of lordosis behavior in rats is progesterone-dependent. Neuropeptides 10:55–65.

Gray EG. 1959. Electron microscopy of synaptic contacts on dendrite spines of the cerebral cortex. Nature 183:1592–1593.

Griffin GD, Flanagan-Cato LM. 2008. Estradiol and progesterone differentially regulate the dendritic arbor of neurons in the hypothalamic ventromedial nucleus of the female rat (Rattus norvegicus). J Comp Neurol 510:631–640.

Honer WG, Hu L, Davies P. 1993. Human synaptic proteins with a heterogeneous distribution in cerebellum and visual cortex. Brain Res 609:9–20.

Hrabovszky E, Kalló I, Hajszán T, Shughrue PJ, Merchenthaler I, Liposits Z. 1998. Expression of estrogen receptor-beta messenger ribonucleic acid in oxytocin and vasopressin neurons of the rat supraoptic and paraventricular nuclei. Endocrinology 139:2600–2604.

Hrabovszky E, Kalló I, Steinhauser A, Merchenthaler I, Coen CW, Petersen SL, Liposits Z. 2004. Estrogen receptor-beta in oxytocin and vasopressin neurons of the rat and human hypothalamus: immunocytochemical and in situ hybridization studies. J Comp Neurol 473:315–333.

Hrabovszky E, Kalló I, Turi GF, May K, Wittmann G, Fekete C, Liposits Z. 2006. Expression of vesicular glutamate transporter-2 in gonadotrope and thyrotrope cells of the rat pituitary. Regulation by estrogen and thyroid hormone status. Endocrinology 147:3818–3825.

Ivell R, Schmale H, Richter D. 1983. Vasopressin and oxytocin precursors as model preprohormones. Neuroendocrinology 37:235–240.

Joseph SA, Piekut DT, Knigge KM. 1981. Immunocytochemical localization of luteinizing hormone-releasing hormone (LHRH) in Vibratome-sectioned brain. J Histochem Cytochem 29:247–254.

Kita H, Oomura Y. 1982. An HRP study of the afferent connections to rat medial hypothalamic region. Brain Res Bull 8:53–62.

Kow LM, Pfaff DW. 2004. The membrane actions of estrogens can potentiate their lordosis behavior-facilitating genomic actions. Proc Natl Acad Sci U S A 101:12354–12357.

Kow LM, Johnson AE, Ogawa S, Pfaff DW. 1991. Electrophysiological actions of oxytocin on hypothalamic neurons in vitro: neuropharmacological characterization and effects of ovarian steroid hormones. Neuroendocrinology 54:526–535.

LaBelle DR, Cox JM, Dunn-Meynell AA, Levin BE, Flanagan-Cato LM. 2009. Genetic and dietary effects on dendrites in the rat hypothalamic ventromedial nucleus. Physiol Behav 98:511–516.

Landgraf, R, Neumann, ID. 2004. Vasopressin and oxytocin release within the brain: a dynamic concept of multiple and variable modes of neuropeptide communication. Front Neuroendocrinol 25:150–176.

Lim ST, Lim KC, Giuliano RE, Federoff HJ. 2008. Temporal and spatial localization of nectin-1 and l-afadin during synaptogenesis in hippocampal neurons. J Comp Neurol 507:1228–1244.

Ludwig M, Pittman QJ. 2003. Talking back: dendritic neurotransmitter release. Trends Neurosci 26:255–261.

Luiten PGM, Room P. 1980. Interrelations between lateral, dorsomedial and ventromedial hypothalamic nuclei in the rat. An HRP study. Brain Res 190:321–332.

Madeira MD, Ferreira-Silva L, Paula-Barbosa MM. 2001. Influence of sex and estrus cycle on the sexual dimorphisms of the hypothalamic ventromedial nucleus: stereological evaluation and Golgi study. J Comp Neurol 432:329–345.

Magistretti PJ, Morrison JH. 1988. Noradrenaline- and vasoactive intestinal peptide-containing neuronal systems in neocortex: functional convergence with contrasting morphology. Neuroscience 24:367–378.

McCarthy MM, Kleopoulos SP, Mobbs CV, Pfaff DW. 1994. Infusion of antisense oligodeoxynucleotides to the oxytocin receptor in the ventromedial hypothalamus reduces estrogen-induced sexual receptivity and oxytocin receptor binding in the female rat. Neuroendocrinology 59:432–440.

Meisel RL, Pfaff DW. 1984. RNA and protein synthesis inhibitors: effects on sexual behavior in female rats. Brain Res 12:187–193.

Millhouse OE. 1973a. Certain ventromedial hypothalamic afferents. Brain Res 55:89–105.

Millhouse OE. 1973b. The organization of the ventromedial hypothalamic nucleus. Brain Res 55:71–87.

Mills RH, Sohn RK, Micevych PE. 2004. Estrogen-induced mu-opioid receptor internalization in the medial preoptic nucleus is mediated via neuropeptide Y-Y1 receptor activation in the arcuate nucleus of female rats. J Neurosci 24: 947–955.

Morris JF, Pow DV. 1991. Widespread release of peptides in the central nervous system: quantitation of tannic acid-captured exocytoses. Anat Rec 231:437–445.

Navarro-Quiroga I, Hernandez-Valdes M, Lin SL, Naegele JR. 2006. Postnatal cellular contributions of the hippocampus subventricular zone to the dentate gyrus, corpus callosum, fimbria, and cerebral cortex. J Comp Neurol 497:833–845.

Nishizuka M, Pfaff DW. 1989. Intrinsic synapses in the ventromedial nucleus of the hypothalamus: an ultrastructural study. J Comp Neurol 286:260–268.

O'Donohue TL, Crowley WR, Jacobowitz DM. 1979. Biochemical mapping of the noradrenergic ventral bundle projection sites: evidence for a noradrenergic–dopaminergic interaction. Brain Res 172:87–100.

Palkovits M. 1982. Neuropeptides in the median eminence: their sources and destinations. Peptides 3:299–303.

Peters A, Palay SL, Webster HF. 1991. The fine structure of the nervous system. Oxford: Oxford University Press.

Peters JH, McDougall SJ, Kellett DO, Jordan D, Llewellyn-Smith IJ, Andresen MC. 2008. Oxytocin enhances cranial visceral afferent synaptic transmission to the solitary tract nucleus. J Neurosci 28:11731–11734.

Pfaff DW. 1989. Features of a hormone-driven defined neural circuit for a mammalian behavior. Principles illustrated, neuroendocrine syllogisms, and multiplicative steroid effects. Ann N Y Acad Sci 563:131–147.

Pfaff D, Keiner M. 1973. Atlas of estradiol-concentrating cells in the central nervous system of the female rat. J Comp Neurol 151:121–158.

Ponzio TA, Ni Y, Montana V, Parpura V, Hatton GI. 2006. Vesicular glutamate transporter expression in supraoptic neurones suggests a glutamatergic phenotype. J Neuroendocrinol 18: 253–265.

Quinones-Jenab V, Jenab S, Ogawa S, Adan RA, Burbach JP, Pfaff DW. 1997. Effects of estrogen on oxytocin receptor messenger ribonucleic acid expression in the uterus, pituitary, and forebrain of the female rat. Neuroendocrinology 65:9–17.

Rainbow TC, McGinnis MY, Davis PG, McEwen BS. 1982. Application of anisomycin to the lateral ventromedial nucleus of the hypothalamus inhibits the activation of sexual behavior by estradiol and progesterone. Brain Res 233: 417–423.

Sabatier N, Rowe I, Leng G. 2007. Central release of oxytocin and the ventromedial hypothalamus. Biochem Soc Trans 35:1247–1251.

Sakamoto H, Matsuda K, Hosokawa K, Nishi M, Morris JF, Prossnitz ER, Kawata M. 2007. Expression of G protein-coupled receptor-30, a G protein-coupled membrane estrogen receptor, in oxytocin neurons of the rat paraventricular and supraoptic nuclei. Endocrinology 148: 5842–5850.

Schumacher M, Coirini H, Pfaff DW, McEwen BS. 1990. Behavioral effects of progesterone associated with rapid modulation of oxytocin receptors. Science 250:691–694.

Simerly RB, Swanson LW. 1988. Projections of the medial preoptic nucleus: a Phaseolus vulgaris leucoagglutinin anterograde tract-tracing study in the rat. J Comp Neurol 270: 209

Simerly RB, Chang C, Muramatsu M, Swanson LW. 1990. Distribution of androgen and estrogen receptor mRNA-containing cells in the rat brain: an in situ hybridization study. J Comp Neurol 294:76b–95.

Sofroniew MV, Schrell U. 1981. Evidence for a direct projection from oxytocin and vasopressin neurons in the hypothalamic paraventricular nucleus to the medulla oblongata: immunohistochemical visualization of both the horseradish peroxidase transported and the peptide produced by the same neurons. Neurosci Lett 22:211–217.

Stern JE, Armstrong WE. 1998. Reorganization of the dendritic trees of oxytocin and vasopressin neurons of the rat supraoptic nucleus during lactation. J Neurosci 18:841–853.

Swanson LW, Sawchenko PE, Wiegand SJ, Price JL. 1980. Separate neurons in the paraventricular nucleus project to the median eminence and to the medulla or spinal cord. Brain Res 198:190–195.

Tribollet E, Barbaris C, Jard S, Dubois-Dauphin M, Dreifuss JJ. 1988. Localization and pharmacological characterization of high affinity binding sites for vasopressin and oxytocin in the rat brain by light microscopic autoradiography. Brain Res 442:105–118.

Watts AG, Swanson LW, Sanchez-Watts G. 1987. Efferent projections of the suprachiasmatic nucleus: I. Studies using anterograde transport of Phaseolus vulgaris leucoagglutinin in the rat. J Comp Neurol 258:204–229.

Witt DM, Insel TR. 1992. Central oxytocin antagonism decreases female reproductive behavior. Ann N Y Acad Sci 652:445–447.

Wong P, Gharbawie OA, Luethke LE, Kaas JH. 2008. Thalamic connections of architectonic subdivisions of temporal cortex in grey squirrels (Sciurus carolinensis). J Comp Neurol 510:440–461.

Yoshimura R, Kiyama H, Kimura T, Araki T, Maeno H, Tanizawa O, Tohyama M. 1993. Localization of oxytocin receptor messenger ribonucleic acid in the rat brain. Endocrinology 133:1239–1246.